Supplementary figures and legend

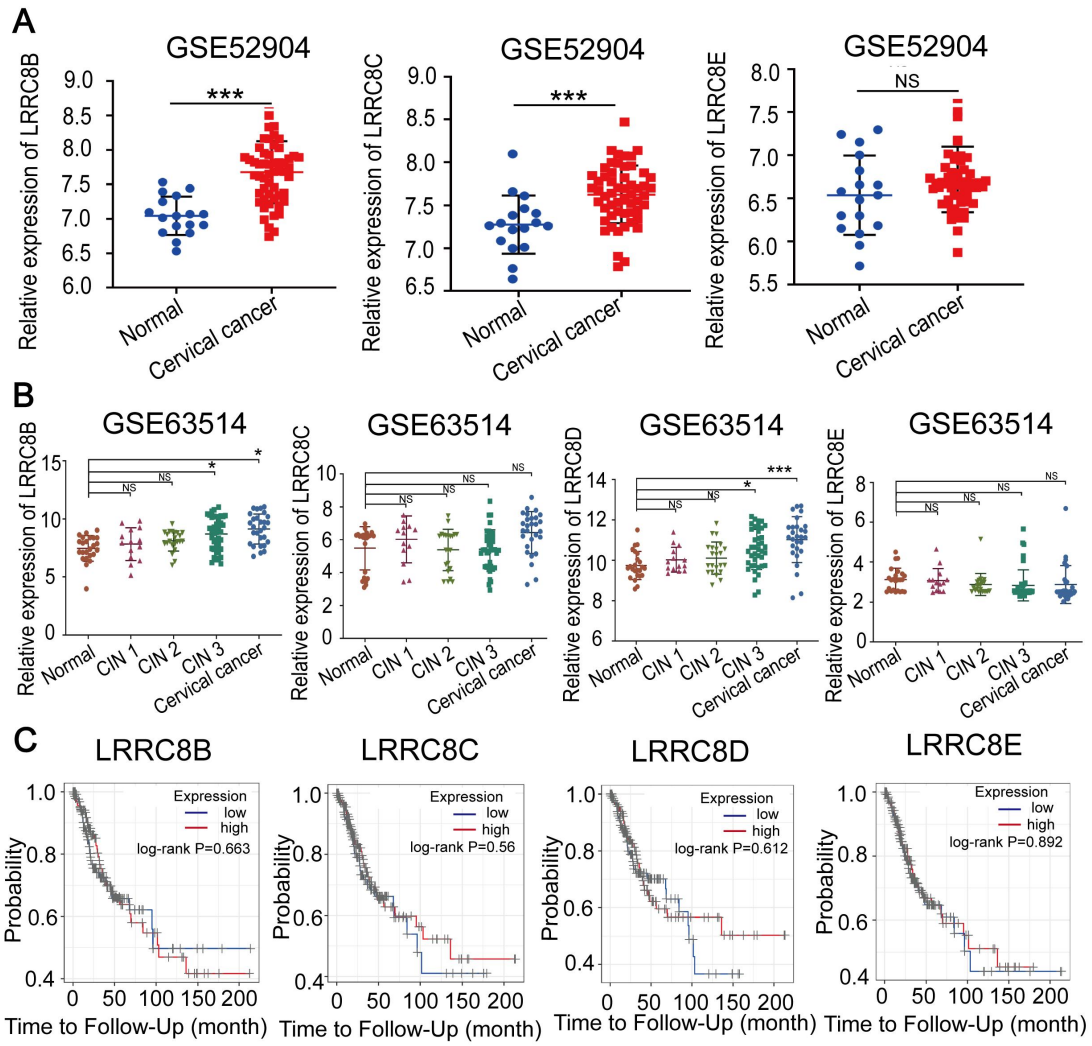

Fig S1. (A and B) Relative RNA levels of LRRC8B, LRRC8C and LRRC8E in CC tissues and normal cervical epithelium in GEO datasets (GSE52904 and GSE63514). **(C)** Kaplan-Meier analysis of CC patients' RFS based on LRRC8B, LRRC8C, LRRC8D, LRRC8E expression by TIMER website. *P<0.05, **P < 0.01, ***P < 0.001, NS, not significant.

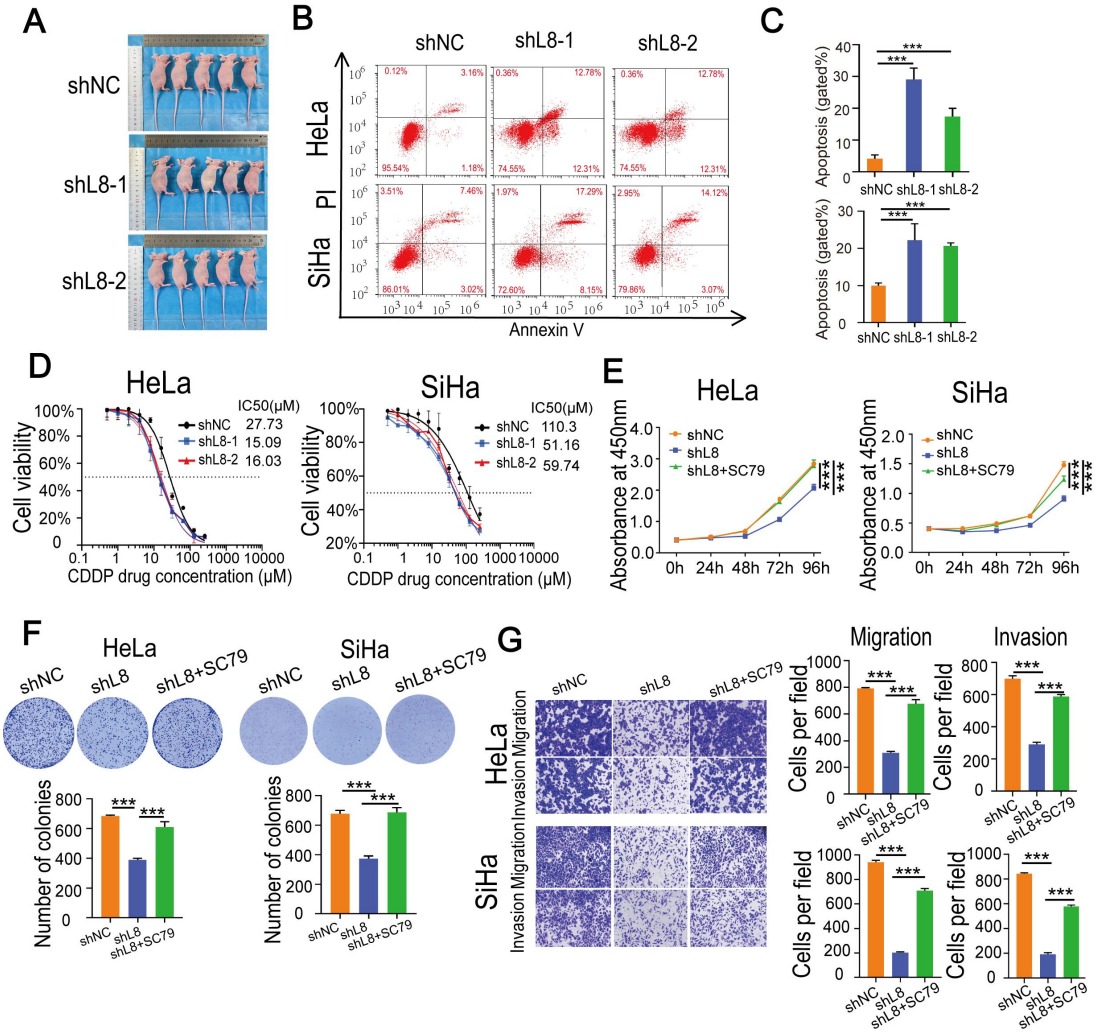

Fig S2. (A) Images of xenograft tumors derived from subcutaneous implantation of LRRC8A knockdown and control cells on nude mice. **(B)** The effect of LRRC8A knockdown on apoptosis of cervical cancer cells. **(C)** Statistical analysis percentage of early-and late-apoptotic cells in LRRC8A knockdown cells. **(D)** Cell viability of control and LRRC8A knockdown cells after treatment with increasing concentrations of cisplatin for 24 h. n = 3. **(E)** The AKT phosphorylation agonist rescues CC cells' proliferation suppressed by LRRC8A depletion. **(F)** SC79 treatment restores the colony formation of CC cells suppressed by LRRC8A knockdown. **(G)** Cell migration and invasion analysis of LRRC8A knockdown in HeLa and SiHa cells with or without SC79 treatment. Scale bar, 200 μm. Data are presented as means ± S.D: ***P < 0.001.

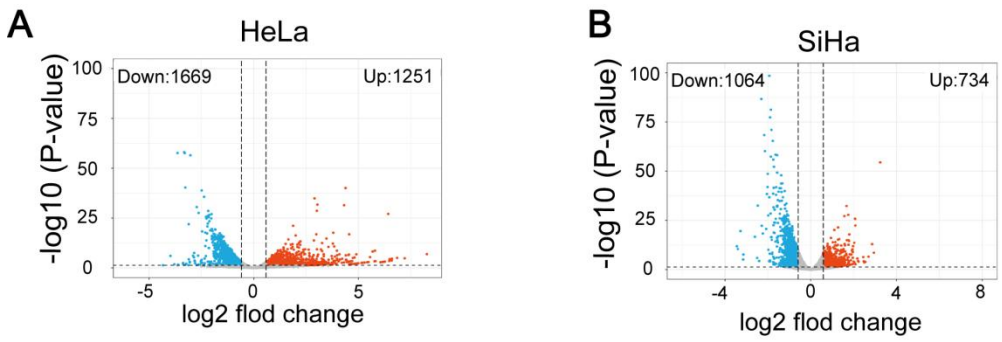

Fig S3. (A) Volcano plot of differentially expressed genes from RNA-seq analysis of NSUN2 knockdown in HeLa cells. **(B)** Volcano plot of differentially expressed genes from RNA-seq analysis of NSUN2 knockdown in SiHa cells.

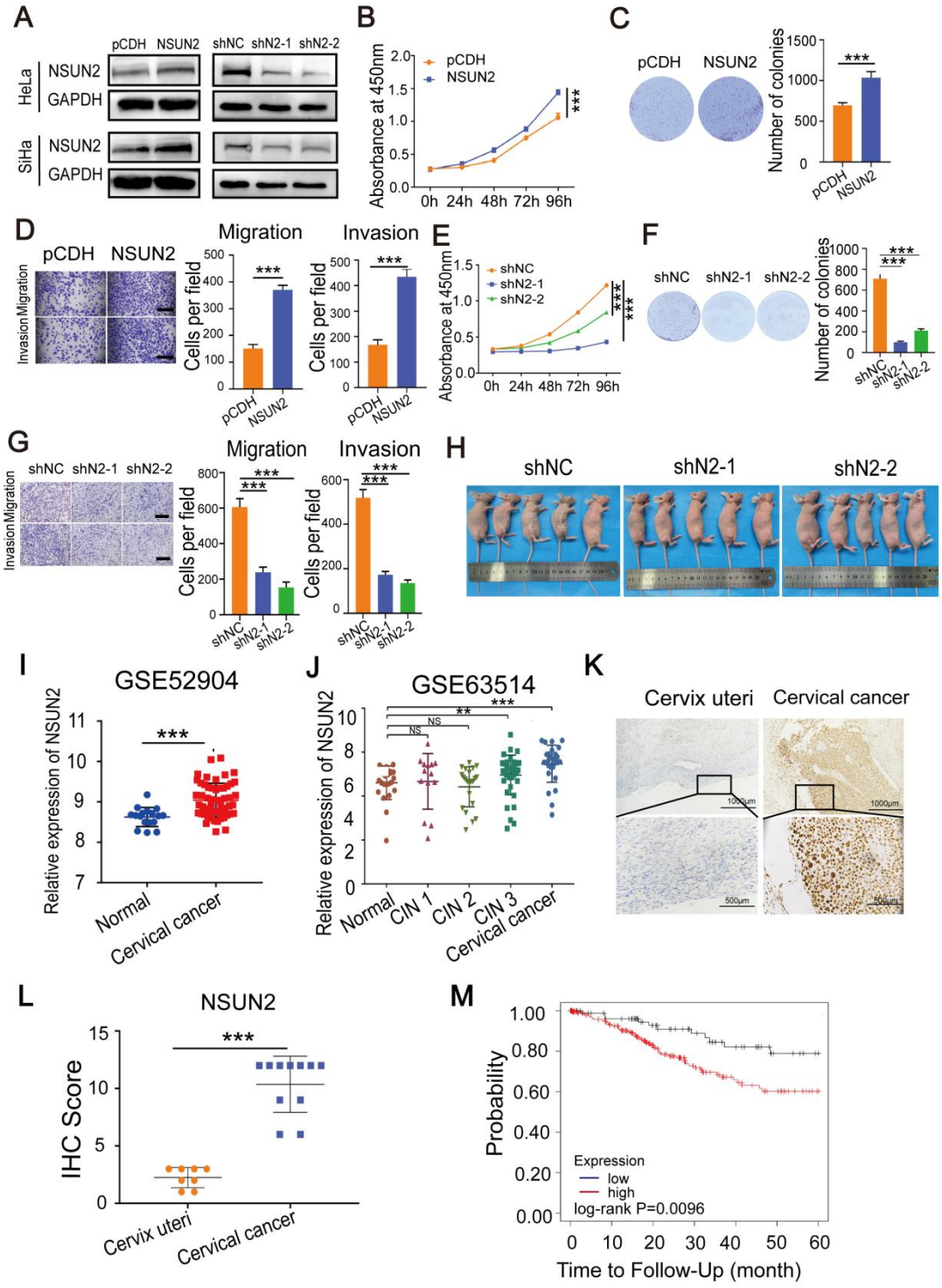

Fig S4. (A) Protein expression of NSUN2 overexpression and knockdown in HeLa and SiHa cells. **(B)** CCK-8 assays showed the proliferation of SiHa cells upon NSUN2 overexpression. **(C)** Cell colony formation of SiHa cells with NSUN2 overexpression. **(D)** Transwell cell migration and invasion analysis of NSUN2 overexpression and control cells. Scale bar, 200 μm. **(E)** The effect of NSUN2 knockdown on cell growth was determined by CCK-8 assays. **(F)**

Colony formation assays were performed in NSUN2 knockdown and control cells. **(G)** Migration and invasion analysis of SiHa cells upon NSUN2 knockdown. Scale bar, 200 μm. **(H)** Images of xenograft tumors derived from subcutaneous implantation of NSUN2 knockdown and control cells on nude mice. **(I and J)** Relative RNA levels of NSUN2 in CC tissues and normal cervical epithelium in GEO datasets (GSE52904 and GSE63514). **(K)** Representative IHC staining images of NSUN2 protein levels in CC tissues and cervical epithelium tissues. Scale bar, upper: 100 μm, lower: 500 μm. **(L)** The quantitative analysis of NSUN2 protein expression in CC tissues and cervical epithelium tissues assessed by IHC staining. **(M)** Kaplan-Meier analysis of CC patients' RFS based on NSUN2 expression. Data are presented as means ± S.D: ***P < 0.001.

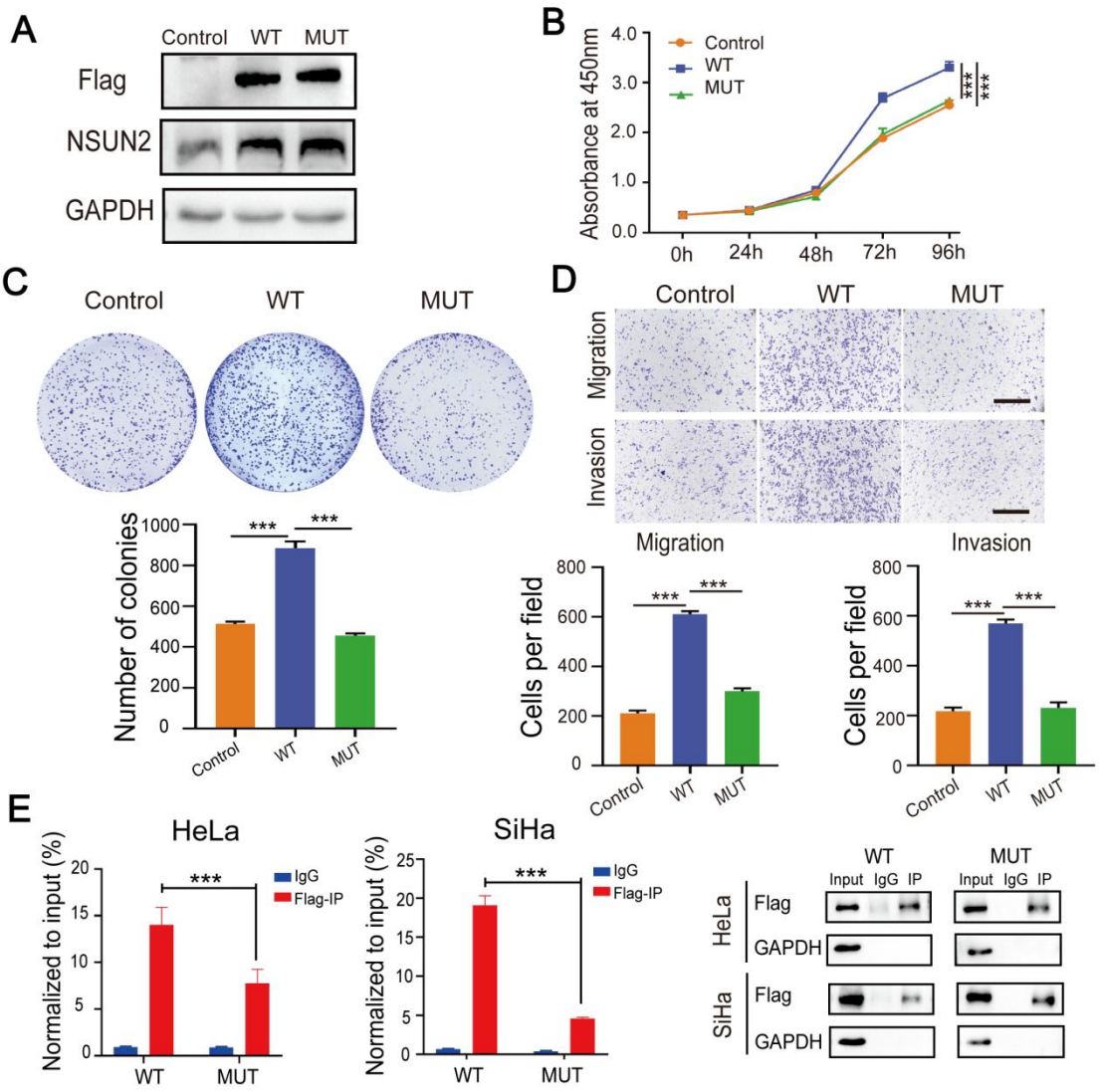

Fig S5. (A) Western blotting assays showed the protein levels of NSUN2 in NSUN2-WT, NSUN2-MUT and control HeLa cells. **(B)** CCK-8 assays of HeLa cells with forced expression of wild-type or catalytic-mutant NSUN2. **(C)** Colony formation assays were performed in CC cells with forced expression of wild-type or mutated NSUN2. **(D)** Transwell cell migration and invasion assay of HeLa cells with forced expression of wild-type or mutated NSUN2. Scale bar, 200 μm. **(E)** RIP-PCR assays detecting the interactions between wild-type or mutated NSUN2 and LRRC8A mRNA. IgG was used as an internal control. GAPDH was used as the negative control in western blot assays. Data are presented as means ± S.D: ***P < 0.001.

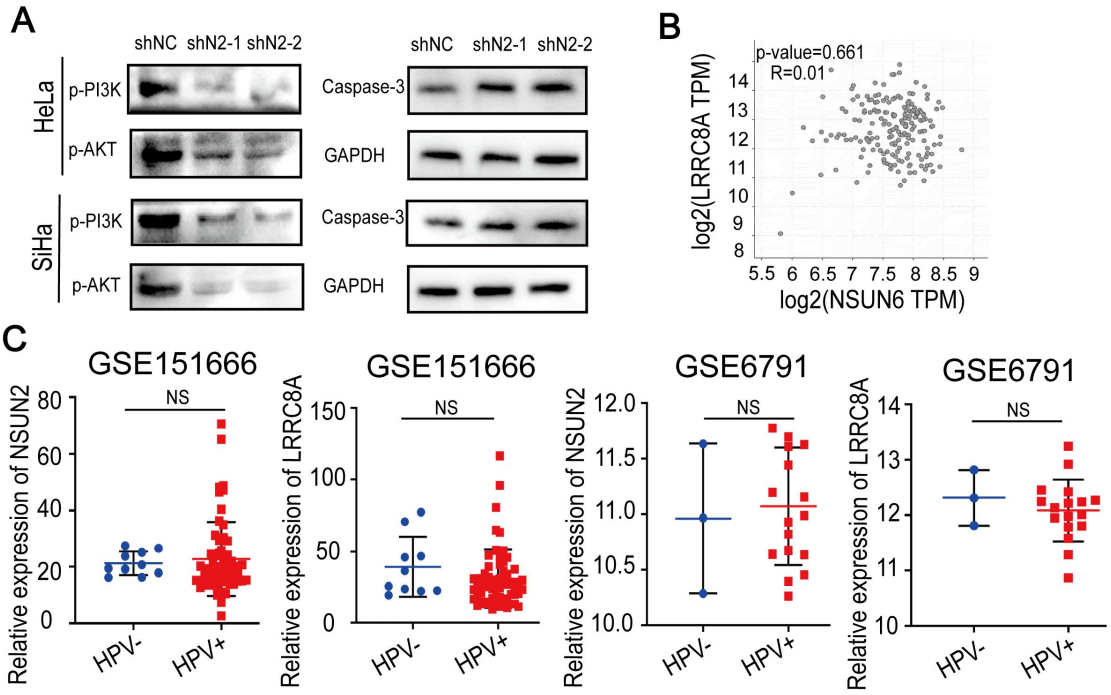

Fig S6. (A) Western blot assays showed protein levels of p-AKT, p-PI3K and Caspase-3 in HeLa and SiHa cells upon NSUN2 knockdown. **(B)** Spearman's correlation analysis between mRNA levels of NSUN6 and LRRC8A in cervical cancer. **(C)** Relative RNA levels of NSUN2 and LRRC8A in HPV negative and HPV positive CC tissues in GEO datasets. NS, not significant.

Supplementary table 1: Sequences of primers and oligos used in this study

	Forword	Reverse
NSUN2	CAAGCTGTTCGAGCACTACTAC	CTCCCTGAGAGCGTCCATGA
GAPDH	CTGGGCTACACTGAGCACC	AAGTGGTCGTTGAGGGCAATG
LRRC8A	TGTGTGCTATGAGAACCGACT	GTGCGCGGGAATTTGAACC
YBX1	GGGGACAAGAAGGTCATCGC	CGAAGGTACTTCCTGGGGTTA
18S	CGATAACGAACGAGACTCTGGC	CGGACATCTAAGGGCATCACA
shLRRC8A-1	CCGGCCGCAACAAGATCGAGAAGATCTCGAGATCTTCTCGATCTTGTTGCGGTTTTTG	AATTCAAAAACCGCAACAAGATCGAGAAGATCTCGAGATCTTCTCGATCTTGTTGCGG
shLRRC8A-2	CCGGCATCTGCTACACCGTCTACTACTCGAGTAGTAGACGGTGTAGCAGATGTTTTTG	AATTCAAAAACATCTGCTACACCGTCTACTACTCGAGTAGTAGACGGTGTAGCAGATG
shNSUN2-1	CCGGGCGTGTTAGAAATCACTTGTTCTCGAGAACAAGTGATTTCTAACACGCTTTTTG	AATTCAAAAAGCGTGTTAGAAATCACTTGTTCTCGAGAACAAGTGATTTCTAACACGC
shNSUN2-2	CCGGGCACACAAATTTAAGTCGAAACTCGAGTTTCGACTTAAATTTGTGTGCTTTTTG	AATTCAAAAAGCACACAAATTTAAGTCGAAACTCGAGTTTCGACTTAAATTTGTGTGC
shYBX1	CCGGCCAGTTCAAGGCAGTAAATATCTCGAGATATTTACTGCCTTGAACTGGTTTTTG	AATTCAAAAACCAGTTCAAGGCAGTAAATATCTCGAGATATTTACTGCCTTGAACTGG